JOURNAL OF
HYDRO-METEOROLOGY

Research Article

Experimental optimization to enhance oil removal efficiency from water using carbonized rambutan peel

Trinh Trong Nguyen[1], Nguyen Dinh Loc[1], Le Huy Ba[2], Thai Van Nam[1]*

[1] HUTECH Institute of Applied Sciences, HUTECH University, Ho Chi Minh City, Vietnam; tt.nguyen@hutech.edu.vn; lochenni@gmail.com; tv.nam@hutech.edu.vn
[2] Faculty of Biology and Environment, Ho Chi Minh City University of Industry and Trade, 140 Le Trong Tan, Ho Chi Minh 700000, Viet Nam; lhuyba@gmail.com

*Corresponding author: tv.nam@hutech.edu.vn; Tel: +84–945007990

Received: 15 October 2023; Accepted: 27 November 2023; Published: 25 March 2024

Abstract: In this study, the objective was to employ experimental design in order to optimize the efficiency of diesel oil removal from water using activated carbon sourced from rambutan peel. A central composite design was utilized to investigate the impact of contact time, adsorbent dosage, initial oil concentration, and pH on both the removal efficiency and oil adsorption capacity across 30 different experimental designs. The analysis of activated carbon properties derived from rambutan peel revealed a BET surface area of 786.014 m2/g, a BJH adsorption cumulative pore volume of 0.054 cm3/g, and an average BJH adsorption pore diameter of 55.243 nm. The quadratic model was employed to estimate the mathematical relationship between the removal efficiency and adsorption capacity of diesel oil in relation to the four key independent variables. The ANOVA analysis demonstrates F-values of 12.36 and 39.92 for the respective models, both exhibiting ρ-values < 0.05. The predicted values closely align with experimental results, showcasing R2 values of 92.02% for removal efficiency and 97.39% for adsorption capacity. The investigation anticipates that, based on the analysis of 87 solutions, optimal conditions of 70.60 minutes of contact time, 0.25 g/g adsorbent dosage, 0.97% v/v initial oil concentration, and a pH of 6.20 will yield a maximum removal efficiency of 72.12% and a maximum adsorption capacity of 5.3570 g/g. This combination of factors achieves a desirability rating of 0.741.

Keywords: Activated carbon; Diesel oil; Materials science; Modeling; Rambutan peel.

1. Introduction

Contaminated water containing oil has a worldwide impact on the quality of water and underwater ecosystems, resulting in serious health repercussions [1]. Techniques for oil elimination in aquatic environments can be sorted into in-situ combustion, chemical approaches (solidification and dispersion), biological methodologies, and physical means (such as skimming and absorbents) [2]. Within these options, oil adsorbents continue to be the favored method for oil cleanup due to their swiftness, simplicity, environmental sustainability [3], and cost-effectiveness. The selection of the adsorbent material is contingent on factors like availability, cost, and safety considerations [4]. Among these categories, adsorbent materials originating from natural organic sources offer notable benefits when compared to others, particularly in regard to their environmental compatibility in marine settings and their lightweight characteristics, which facilitate effortless retrieval and reuse [5].

Activated carbon, produced through carbonization, is employed for the adsorption of a wide range of substances [6]. Activated carbon derived from plant biomass is especially preferred due to its abundant and easily accessible origin, leading to notably reduced manufacturing expenses when compared to commercially available activated carbon [7]. Consequently, numerous distinct activated carbon materials have been manufactured from diverse plant-based sources, including coconut shells [7], coconut coir [8], corn cobs [9], safou seeds [10], oil palm endocarp [11] and rambutan peel [12]. Some activated carbon materials of natural origin have been recently used for oil absorption, such as carbonized pith bagasse [13], carbonized rice husk [14], activated carbon tablets from corncobs [6], mango shell activated carbon [15], and corn cobs activated carbon [9].

Rambutan peel (RP) is considered an agricultural waste with a substantial cellulose content, amounting to 24.28 % [16], rendering it a cost-effective and suitable economical material for the adsorption of oil in water. In this study, the rambutan peel will be chosen as the primary material to produce low-cost and environmentally friendly oil-absorbent substances. The employment of statistical experimental design approaches within the adsorption process has been put into practice to reduce process variability and minimize resource demands [17]. Response Surface Methodology (RSM) is a mathematical and statistical method utilized for experimental design, modeling, assessing the relative importance of independent variables, and determining optimal conditions for desired outcomes [18]. Grounded in Central Composite Design (CCD), RSM has been broadly utilized for determining the best conditions in multivariate systems [19]. More recently, it has been effectively used to optimize parameters in various wastewater treatment processes [20].

Presently, there have been no investigations that have employed Response Surface Methodology (RSM) with Central Composite Design (CCD) to optimize parameters for the removal of oil from water utilizing chemically activated carbon derived from RP. The use of RMS via CCD helps fine-tune the factors influencing the adsorption process to determine optimal values for enhancing the oil adsorption and removal capabilities of RPAC under realistic environmental conditions. The objective of this study will focus on experiment optimization to enhance the efficiency of oil removal from water using carbonized rambutan peel through a surface response method based on CCD.

2. Material and methods

2.1. Materials

Rambutan peel was procured from the primary market located in Ho Chi Minh City, Vietnam. Diesel oil (DO) 0.05 S was acquired from Petrolimex Aviation in Ho Chi Minh City, Vietnam, and it exhibited a specific gravity at 15^{o}C ranging from 820 to 860 kg/m^{3}. Potassium hydroxide, n-Hexane, and sodium sulfate anhydrous were obtained from Xilong Scientific Co., Ltd. in Shenzhen, China. Hydrochloric acid (c(HCl) = 0.1 mol/l or 0.1 N) was supplied by Merck in Germany.

2.2. Preparation of adsorbent

Rambutan peel underwent a series of steps, including rinsing with deionized water, drying at 105^{o}C for 24 hours, grinding to achieve a particle size of 1-2 mm, and subsequent carbonization at 550^{o}C for 2 hours in purified nitrogen (99.99 %). The resultant product was subjected to impregnation with KOH pellets at a 1:2 ratio [21]. These KOH pellets were dissolved in deionized water to form a 1 N KOH solution, and the mixture was soaked for a period of 24 hours. Afterward, it was dried for 24 hours at 105^{o}C to eliminate moisture, followed by activation in a muffle furnace at 550^{o}C for 1 hour. The resulting rambutan peel activated carbon (RPAC) was subsequently cooled, treated with a 0.1 N HCl solution to

eliminate ash content, rinsed with distilled water until achieving a pH range of 6-7, dried at 105^{o}C for 2 hours, crushed, sieved into various particle sizes, and finally stored in a desiccator for future use.

2.3. Characterization of adsorbent

Brunauer-Emmett-Teller (BET) theory is used to measure the surface area of RP and RPAC. The solid sample is cooled under vacuum to cryogenic temperature using liquid nitrogen. Nitrogen gas is incrementally dosed to the sample, allowing equilibration of relative pressure (P/P_0) after each dose. The BET equation involves a linear plot of $1/((P_0/P)-1)$ vs. P/P0, typically within the range of 0.05 to 0.35 for most solids. From this plot, the weight of nitrogen for a monolayer (Wm) is determined, enabling calculation of the total surface area using the BET equation and the nitrogen molecule's known cross-sectional area [22].

$$\frac{1}{W\left(\frac{P_0}{P}-1\right)}=\frac{1}{W_mC}+\left(\frac{C-1}{W_mC}\right)\frac{P}{P_0} \quad (1)$$

The weight of gas adsorbed at a relative pressure of P/P_0 is represented by W, while Wm signifies the weight of the adsorbate forming a monolayer of surface coverage. The term C, known as the BET C constant, correlates with the energy of adsorption within the initial adsorbed layer. Therefore, its value serves as an indicator of the strength of interactions between the adsorbent and adsorbate [22].

To ascertain the pore volume and distribution of pore sizes, the gas pressure is gradually increased until all pores are saturated with nitrogen molecules. Subsequently, the pressure is gradually decreased, causing the condensed nitrogen gas to evaporate from the system. Analyzing the adsorption and desorption isotherms provides insights into both pore volume and the distribution of pore sizes [22]. The RPAC produced under optimal conditions was evaluated for its surface area, pore volume, and average pore diameter using the Micromeritics® TriStar II Plus Version 3.03.

Scanning Electron Microscope (SEM) analysis was conducted using the JSM-IT500 InTouchScope™ Scanning Electron Microscope.

2.4. Approach for assessing the effectiveness of oil adsorption

In each trial, the quantity of oil adsorbed per gram of adsorbent at equilibrium is represented as q_e (g/g), at a given time t is denoted as q_t (g/g), and the adsorption efficiency is calculated using the subsequent equation [21]:

$$q_e=\frac{(C_o-C_e)\times V}{M} \quad (2)$$

$$q_t=\frac{(C_o-C_t)\times V}{M} \quad (3)$$

$$\%\ \text{Effective removal}=\frac{(C_o-C_e)\times 100}{C_o} \quad (4)$$

where C_o stands for the initial oil concentration (mg/L); C_e is the concentration at equilibrium (mg/L); C_t denotes the oil concentration at time t (mg/L); V represents the solution volume (ml); and M is the mass of the adsorbent used.

2.5. Experimental design for optimization

The CCD encompasses 2^n factorial runs, along with 2n axial runs and n_c center runs. The center points serve to evaluate experimental error and data reproducibility, while the axial points ensure rotatability to maintain a constant variance of model predictions equidistant

from the design center [23]. Hence, as per [24], the necessary number of experimental runs can be determined using equation (5).

$$N = 2^n + 2n + n_c = 2^4 + 2 \times 4 + 6 = 30 \quad (5)$$

where N = Total number of experimental runs, n = number of independent variables (factors), and n_c = number of center points. This study considered four independent variables: contact time (A), adsorbent dosage (B), initial oil concentration (C), and pH (D). The dependent parameters or responses were removal efficiency (Y_1) and adsorption capacity (Y_2). The RSM model analysis utilized the CCD from Design-Expert 13. The optimal values (Center) of the factors influencing the oil adsorption process of RPAC will be selected based on the research findings of [12] to incorporate into the optimal experimental design. The ranges of the independent variables are presented in Table 1.

Table 1. Factors and levels tested for experimental design.

	Symbol	Low	Center	High	Unit
Level		-1	0	1	
Contact time	A	50	60	70	min
Adsorbent dosage	B	0.25	0.5	0.75	g
Initial oil concentration	C	0.75	1.0	1.25	% v/v
pH	D	5.0	6.0	7.0	

3. Results and discussion

3.1. Characteristics of the adsorbent

The BET surface area of RPAC was 786.014 m^2/g. The increased BET surface area in RPAC indicated more active sites, enhancing oil uptake [25]. The pore volume is 0.054 cm^3/g, while the pore diameter increased is 55.243 nm. The surface structure of raw RP exhibits uniform fiber-like crystal bonds and small pores, indicative of mineral presence (Figure 1a). This surface primarily consists of a lignocellulose network and a fiber matrix containing lignin, cellulose, volatile organic compounds, and hemicellulose. Following carbonization and alkaline treatment, RPAC's surface displays uneven, rough, and rugged structures with larger, deeper existing pores, accompanied by an increase in their number on the material's surface (Figure 1b). The KOH-C reaction enhances pore development during activation, thereby increasing surface area and adsorption capacity. A nearly heterogeneous pore structure pattern is also observable on the RPAC surface.

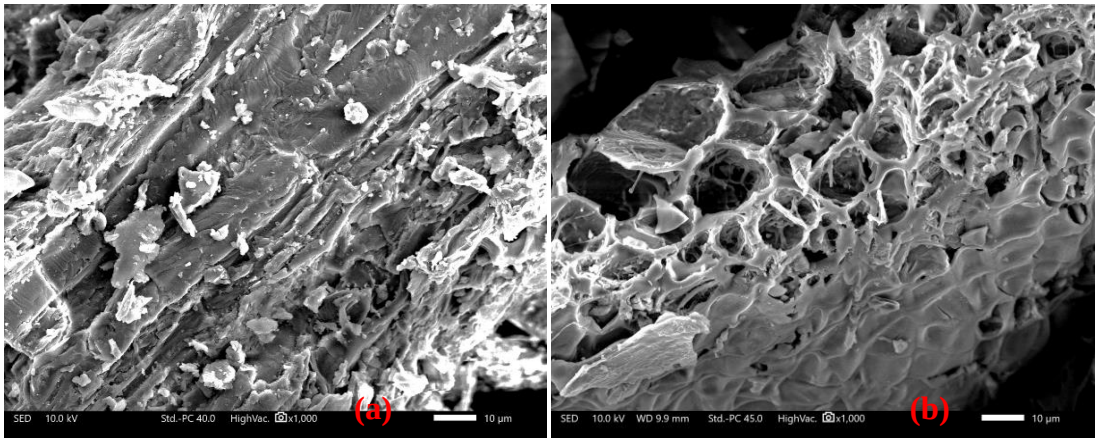

Figure 1. SEM images of raw RP (a) and RPAC (b).

3.2. Experimental design

Table 2 shows that the oil removal efficiency (Y_1) of RPAC ranged from 48.05% to 86.20%, with the highest and lowest values recorded. Similarly, the oil adsorption capacity (Y_2) ranged from 1.1679 g/g to 5.9876 g/g.

Table 2. Experimental design matrix of RPAC.

Run	Factors				Responses			
	Contact time (min)	Adsorbent dosage (g)	Initial oil concentration (% v/v)	pH	Removal efficiency (%)		Adsorption capacity (g/g)	
	(A)	(B)	(C)	(D)	Experimental	Predicted	Experimental	Predicted
1	60	0.5	1	6	74.52	74.65	3.2296	3.2500
2	70	0.75	1.25	5	72.40	71.06	2.6236	2.3400
3	50	0.75	1.25	7	70.20	70.67	2.5372	2.3800
4	70	0.75	0.75	7	72.21	73.47	1.5692	1.5700
5	70	0.25	1.25	7	54.83	54.82	5.9756	5.9500
6	60	0.5	0.5	6	55.21	52.13	1.1926	1.0300
7	60	0.5	1	6	75.38	74.65	3.2788	3.2500
8	70	0.75	0.75	5	61.61	64.78	1.3477	1.4100
9	60	0.5	1	6	73.90	74.65	3.2076	3.2500
10	70	0.25	1.25	5	54.00	55.35	5.8600	5.7900
11	50	0.25	0.75	7	55.23	57.86	3.6416	3.8000
12	50	0.25	1.25	7	55.13	50.63	5.9876	5.6400
13	60	0.5	1.5	6	48.05	51.18	3.2244	3.7900
14	50	0.75	1.25	5	74.01	68.82	2.7064	2.3200
15	70	0.25	0.75	7	65.95	69.81	4.3152	4.4300
16	60	0.5	1	6	75.61	74.65	3.2988	3.2500
17	50	0.75	0.75	5	53.48	54.78	1.1679	1.0700
18	60	0.5	1	4	50.60	52.62	2.2036	2.5000
19	60	0.5	1	8	62.16	60.18	2.7010	2.8000
20	70	0.25	0.75	5	63.28	64.10	4.1532	4.1900
21	40	0.5	1	6	52.15	58.22	2.2680	2.7200
22	50	0.25	0.75	5	56.97	52.75	3.7220	3.5800
23	50	0.75	0.75	7	65.55	62.87	1.4343	1.2200
24	80	0.5	1	6	78.43	72.41	3.4180	3.3700
25	60	0.5	1	6	78.51	74.65	3.4108	3.2500
26	70	0.75	1.25	7	70.62	73.51	2.5565	2.4200
27	60	0.5	1	6	72.95	74.65	3.1728	3.2500
28	60	0.5	1	6	71.65	74.65	3.1284	3.2500
29	60	1	1	6	86.20	86.25	1.8775	2.2800
30	50	0.25	1.25	5	51.72	51.75	5.6204	5.5000

3.3. Analysis of variance (ANOVA)

The selected model equations for removal efficiency (response Y_1) and adsorption capacity (response Y_2) underwent ANOVA analysis to assess the significance and adequacy of the models. The ANOVA results of the quadratic model, presented in Table 3 and Table 4, indicate that the model equations effectively describe the oil removal performance of RPAC under the experimental conditions. The F-values for the two corresponding models are 12.36 and 39.92, and the ρ -values for both models are < 0.05, demonstrating the significance of both models. Regarding removal efficiency, factors A (ρ = 0.0007), B (ρ < 0.0001), D (ρ = 0.0383), BC (ρ = 0.0022, A^2 (ρ = 0.0087), C^2 (ρ < 0.0001), and D^2 (ρ < 0.0001) significantly influence the response (with p-values less than 0.05 and high F-values) (Table 3). Similarly, for adsorption capacity, factors A (ρ = 0.0205), B (ρ < 0.0001), C (ρ < 0.0001), BC (ρ = 0.043), B^2 (ρ < 0.0001), C^2 (ρ = 0.0026), and D^2 (ρ = 0.022) significantly impact the response (with p-values less than 0.05 and high F-values) (Table 4). Factors that do not have a significant influence (ρ > 0.05) will be removed from the regression equation, as presented in equations (6) and (7).

Table 3. Analysis of variance of regression model for removal efficiency of RPAC.

Source	Sum of Squares	df	Mean Square	F-value	ρ -value
Model	2877.06	14	205.5	12.36	< 0.0001*
A	302.25	1	302.25	18.18	0.0007*
B	459.98	1	459.98	27.67	< 0.0001*

Source	Sum of Squares	df	Mean Square	F-value	ρ -value
C	1.35	1	1.35	0.0811	0.7797
D	85.77	1	85.77	5.16	0.0383*
AB	1.83	1	1.83	0.11	0.7447
AC	60.18	1	60.18	3.62	0.0765
AD	0.357	1	0.357	0.0215	0.8854
BC	225.98	1	225.98	13.59	0.0022*
BD	8.87	1	8.87	0.5333	0.4765
CD	38.91	1	38.91	2.34	0.1469
A2	151.18	1	151.18	9.09	0.0087*
B2	1.57	1	1.57	0.0946	0.7626
C2	917.56	1	917.56	55.19	< 0.0001*
D2	577.61	1	577.61	34.74	< 0.0001*
Residual	249.38	15	16.63		
Lack of Fit	220.56	9	24.51	5.10	
Pure Error	28.82	6	4.80		
Cor Total	3126.44	29			

Note: * = Significant; df = Degree of freedom.

Table 4. Analysis of variance of regression model for adsorption capacity of RPAC.

Source	Sum of Squares	df	Mean Square	F-value	ρ -value
Model	52.35	14	3.74	39.92	< 0.0001*
A	0.6284	1	0.6284	6.71	0.0205*
B	39.01	1	39.01	416.46	< 0.0001*
C	11.45	1	11.45	122.27	< 0.0001*
D	0.1366	1	0.1366	1.46	0.2459
AB	0.0731	1	0.0731	0.78	0.3911
AC	0.0985	1	0.0985	1.05	0.3214
AD	0.0001	1	0.0001	0.0015	0.9692
BC	0.458	1	0.458	4.89	0.043*
BD	0.0061	1	0.0061	0.0653	0.8018
CD	0.0065	1	0.0065	0.0696	0.7955
A2	0.0714	1	0.0714	0.7619	0.3965
B2	4.3	1	4.3	45.94	< 0.0001*
C2	1.22	1	1.22	12.99	0.0026*
D2	0.6113	1	0.6113	6.53	0.022*
Residual	1.41	15	0.0937		
Lack of Fit	1.35	9	0.1503	17.36	
Pure Error	0.0520	6	0.0087		
Cor Total	53.75	29			

Note: * = Significant; df = Degree of freedom

For the model presented in equations (6) and (7) of coded factors, the correlation coefficients R^2 and adjusted R^2 exhibit a high degree of correlation, reaching 92.02 % and 84.58 % for Y_1, and 97.39 % and 94.95 % for Y_2, respectively. This indicates that the regression model closely aligns with the experimental data and effectively reveals the relationships between the independent variables and the response. The coefficients associated with single factors represent the influence of that specific factor, while the coefficients related to two factors depict the interaction between those two factors. The negative coefficients preceding the independent and interaction factors in these equations signify that they exert a diminishing effect on the responses. For the individual effects, three factors, A, B and D, exhibit a positive influence on Y_1 in the sequence of B > A > D, while two factors, A and C, positively impact Y_2 and B adversely affects Y_2 with the order of B > C > A. Concerning interacting effects, BC positively affects Y_1 and adversely affects Y_2. In terms of quadratic effects, A^2, C^2, D^2 negatively impact Y_1 in the order of $C^2 > D^2 > A^2$. Conversely, B^2 has a positive effect, while C^2 and D^2 have negative impacts on Y_2 in the order of $B^2 > C^2 > D^2$. Among these factors, C^2 (as quadratic effects) significantly influences Y_1 (with the highest

F-value of 55.19), while B (as an individual factor) notably affects Y_2 (with the highest F-value of 416.46).

$$Y_1\ (\%) = 74.65 + 3.55A + 5.18B + 1.89D + 3.76BC - 2.33A^2 - 5.75C^2 - 4.56D^2 \quad (6)$$

$$Y_2\ (g/g) = 3.25 + 0.1618A - 1.51B + 0.6908C - 0.1692BC + 0.5124\ B^2 - 0.2093C^2 - 0.1484D^2 \quad (7)$$

The comparison between the predicted removal efficiency and adsorption capacity of RPAC and the observed values is illustrated in Figure 2. The model has successfully captured the correlation between independent variables and dependent parameters or responses, as the results indicate a close match between the predicted values and the actual experimental values.

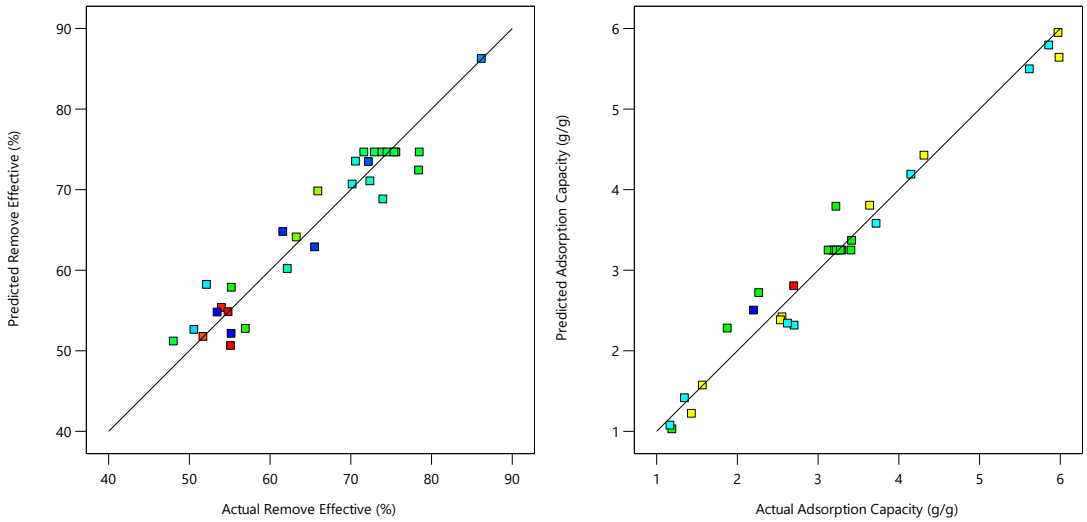

Figure 2. Actual and predicted plot of removal efficiency and adsorption capacity of RPAC.

3.4. Pareto diagram

From the Pareto charts for removal efficiency of RPAC (Figure 3a), it is evident that the adsorbent dosage, contact time, pH of the solution, and the interaction between adsorbent dosage and initial oil concentration are significant and positive standardized effects on RPAC's removal efficiency. Similarly, from the Pareto charts for adsorption capacity of RPAC (Figure 3b), the initial oil concentration, contact time, and pH of the solution significantly positively impact RPAC's adsorption capacity.

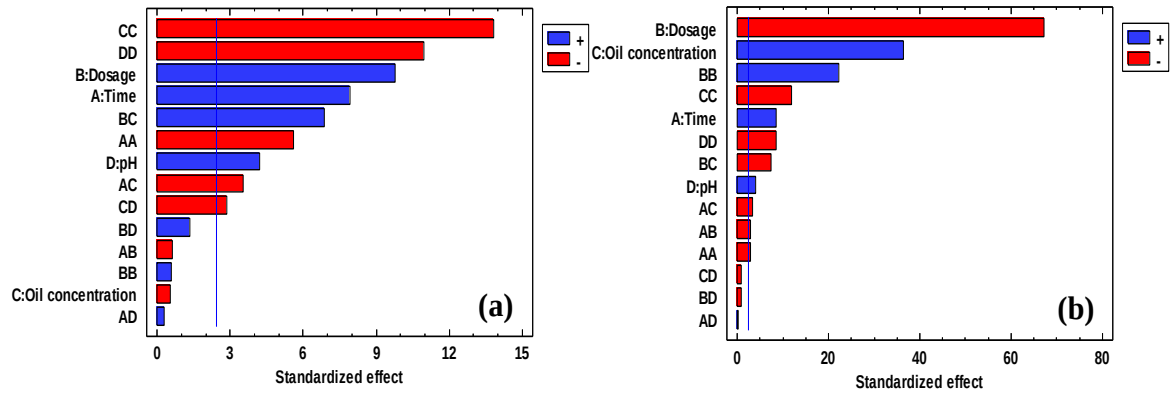

Figure 3. (a) Pareto diagram for removal efficiency of RPAC; (b) Pareto diagram for adsorption capacity of RPAC.

3.5. Response surface analysis

In this segment, the impact of notable interactive effects between the adsorbent quantity (B) and initial oil concentration (C) on the efficiency of elimination and adsorption capability using RPAC is deliberated.

3.5.1. Interaction of adsorbent dosage and initial oil concentration on removal efficiency

Figures 4a,b show contour plots and response surface plots for adsorbent dosage and initial oil concentration on removal efficiency.

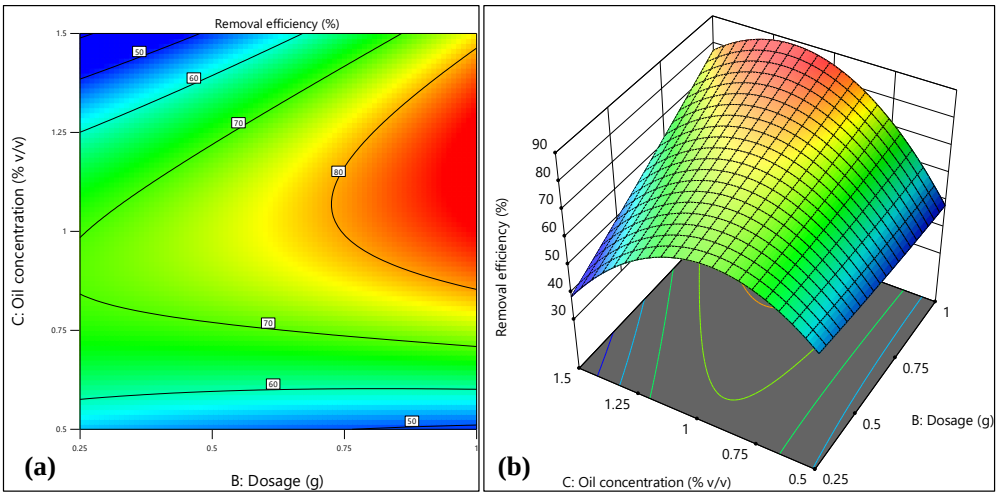

Figure 4. Interaction of adsorbent dosage and initial oil concentration on removal efficiency: (a) Contour plot of adsorbent dosage and initial oil concentration (pH = 6, Contact time = 60 min); (b) Response surface plot of time and dosage (pH = 6, Contact time = 60 min).

As depicted in Figure 4, it is evident that increasing the dosage of the adsorbent does not significantly enhance the removal efficiency when the initial oil concentration is low (0.5% v/v). The RPAC achieves maximum oil removal efficiency of 86.2% at an adsorbent dosage of 1g and an initial oil concentration of 1% v/v. The lowest oil removal efficiency of RPAC (48.5%) occurs at an adsorbent dosage of 0.5g and an initial oil concentration of 1.5% v/v. Increasing the adsorbent dosage from 0.5g to 1g alongside an increase in the initial oil concentration contributes more significantly to the RPAC's removal efficiency. However, with the same adsorbent dosage, excessively high initial oil concentrations lead to a decrease in RPAC's removal efficiency. This can be ascribed to the decrease in the quantity of active sites accessible on the adsorbent's surface responsible for adhering to oil. This discovery corresponds [8] observations, which demonstrated a comparable pattern while employing coconut coir-activated carbon for oil spill remediation.

3.5.2. Interaction of adsorbent dosage and initial oil concentration on adsorption capacity

Figures 5a,b show contour plots and response surface plots for adsorbent dosage and initial oil concentration on adsorption capacity.

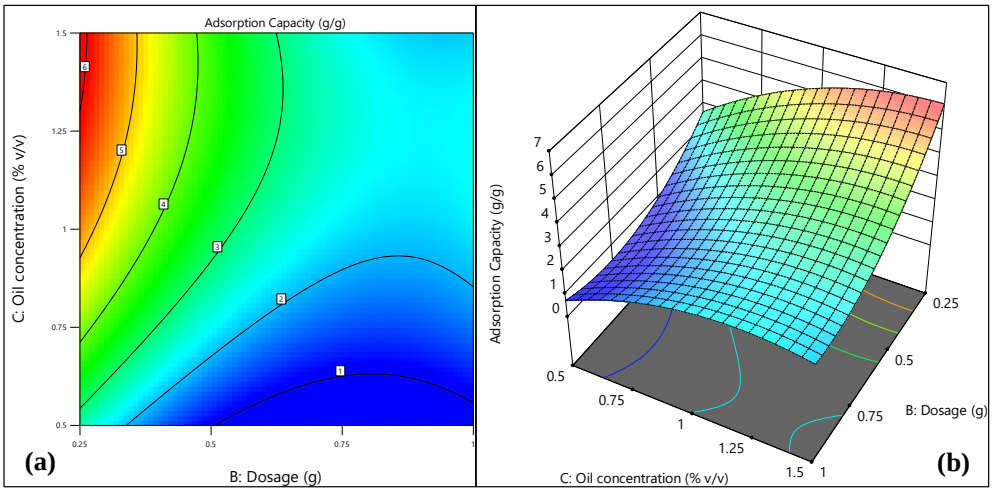

Figure 5. Interaction of adsorbent dosage and initial oil concentration on adsorption capacity: (a) Contour plot of adsorbent dosage and initial oil concentration (pH = 6, Contact time = 60 min); (b) Response surface plot of time and dosage (pH = 6, Contact time = 60 min).

As evident in Figure 5, increasing the adsorbent dosage at the same oil concentration leads to a reduction in RPAC's adsorption capacity. The surplus presence of RPAC in the surroundings might impede the infiltration of oil molecules, restricting their access to active sites on the surface. Consequently, this limitation curtails additional adsorption capacity and hampers the complete elimination of oil. A similar trend was observed in a study by [26], wherein the adsorption capacity initially rose as the adsorbent dosage increased from 0.5 g to 1.5g, but then exhibited a declining pattern. This decline could be attributed to the compression of fibers at higher dosages, potentially impeding the uniform penetration of oil into the fibers. Increasing the initial oil concentration from 0.5% v/v to 1.5% v/v at different dosages consistently demonstrates an elevation in RPAC's oil adsorption capacity, particularly at lower adsorbent dosages. Specifically, the RPAC's oil adsorption capacity peaks when the initial oil concentration is 1.25% v/v, coupled with an adsorbent dosage of 0.25g.

3.6. Optimization of the adsorption process

Optimizing each response will help determine the optimal conditions for the influencing factors in the oil adsorption process of RPAC. Table 5 shows that to maximize the removal efficiency to 88.89 %, the optimal conditions for the factors (i.e., contact time, adsorbent dosage, initial oil concentration, and pH) are 66.45 min, 1 g/g, 1.09% v/v, and 6.33, respectively. To achieve a maximum adsorption capacity of 6.0940 g/g, the optimal conditions for the factors (i.e., contact time, adsorbent dosage, initial oil concentration, and pH) are 63.64 min, 0.25 g/g, 1.36% v/v, and 6.43, respectively.

Table 5. Optimization of the adsorption process to achieve the goal of maximizing removal efficiency and adsorption capacity.

Factor	Low	High	Optimum	
			Maximizing removal efficiency	Maximizing adsorption capacity
- Contact time (min)	40	80	66.45	63.64
- Adsorbent dosage (g)	0.25	1.0	1.0	0.25
- Initial oil concentration (% v/v)	0.5	1.5	1.09	1.36
- pH	4.0	8.0	6.33	6.43
Responses				
- Removal efficiency (%)			88.89	
- Adsorption capacity (g/g)				6.0940

Multiple response optimization aims to find the best combination of factors to maximize both oil removal efficiency and adsorption capacity simultaneously. This is done by finding the highest value of a particular desirability measure. Table 6 displays the factor settings that achieve the highest desirability values within the specified range. After evaluating 87 solutions, the optimal conditions were determined: contact time of 70.60 min, adsorbent dosage of 0.25 g/g, initial oil concentration of 0.97% v/v, and a pH of 6.20. Under these conditions, the optimal oil removal efficiency is 72.12%, and the optimal oil adsorption capacity is 5.3570 g/g.

Table 6. Optimization of the adsorption process to achieve the goal of maximizing removal efficiency and adsorption capacity.

Factor	Low	High	Optimum
- Contact time (min)	40	80	70.60
- Adsorbent dosage (g)	0.25	1.0	0.25
- Initial oil concentration (% v/v)	0.5	1.5	0.97
- pH	4.0	8.0	6.20
Responses			
- Removal efficiency (%)	48.05	86.20	72.12
- Adsorption capacity (g/g)	1.1679	5.9876	5.3570

Based on the results in Table 5 and Table 6, the maximum predicted oil adsorption capacity (RPAC) is 6.0940 g/g, and the target for optimizing multiple responses is 5.3570 g/g. These results are higher than the oil adsorption capacity of pyrolyzed rice husk (5.02 g/g) [27] as well as activated carbon from coconut husk fibers (4,859.5 mg/g) [8]. However, they are lower than the Gas oil adsorption capacity of activated carbon from barley straw [13].

4. Conclusion

Activated carbon derived from rambutan peel demonstrates effective oil removal from water. The main conclusions are as follows: (1) The carbonization and KOH activation processes result in a more porous structure with a BET surface area of 786.014 m^2/g, BJH adsorption cumulative pore volume of 0.054 cm^3/g, and BJH adsorption average pore diameter of 55.243 nm. Raw RP's surface structure shows uniform fiber-like crystal bonds and small pores, indicating mineral presence. After carbonization and alkaline treatment, RPAC's surface exhibits uneven, rough, and rugged structures with larger, deeper pores, accompanied by an increased number of pores on the material's surface. (2) ANOVA analysis indicates F-values of 12.36 and 39.92 for the respective models, both displaying ρ-values < 0.05. The predicted values closely align with experimental results, demonstrating R^2 values of 92.02% for removal efficiency and 97.39% for adsorption capacity. In terms of diesel oil removal efficiency, the significant influential factors follow the sequence of B > A > D for contact time (A), adsorbent dosage (B), and pH (D). Meanwhile, adsorption capacity is influenced by contact time (A), adsorbent dosage (B), and initial oil concentration (C) in the order of B > C > A. (3) The response surface plots, Pareto chart, and variance analysis indicated the most significant antagonistic interaction between adsorbent dosage and initial oil concentration concerning removal efficiency (F-value = 13.59, ρ-value = 0.0022) and adsorption capacity (F-value = 4.89, ρ-value = 0.043). (4) The study predicts a maximum removal efficiency of 72.12% and a maximum adsorption capacity of 5.3570 g/g under specific conditions: 70.60 min of contact time, 0.25 g/g adsorbent dosage, 0.97% v/v initial oil concentration, and a pH of 6.20, with a desirability rating of 0.741 based on the analysis of 87 solutions.

Author contribution statement: Defining and developing the research idea and researchframework: T.V.N., L.H.B.; Collecting data and literature, data analysis and synthesis: T.T.N., N.D.L.; Experimental research: T.T.N., N.D.L.; Drafting the manuscript: T.T.N.; Manuscript editing and revision: T.V.N., L.H.B.

Acknowledgement: This research was fully funded by HUTECH University under grant number 25/HĐ-ĐKC and the AKIHIKO IKAI Family Scholarship Fund.

Competing interest statement: The authors declare that this article was the work of theauthors, has not been published elsewhere, has not been copied from previous research; therewas no conflict of interest within the author group.

Reference

1. Kolokoussis, P.; Karathanassi, V. Oil spill detection and mapping using sentinel 2 imagery. *J. Mar. Sci*. **2018**, *6*, 1–12.
2. Alaa El-Din, G.; Amer, A.A.; Malsh, G.; Hussein, M. Study on the use of banana peels for oil spill removal. *Alex. Eng. J*. **2018**, *57*, 2061–2068.
3. El-Nafaty, U.A.; Muhammad, I.M.; Abdulsalam, S. Biosorption and kinetic studies on oil removal from produced water using banana peel. *Civ. Environ. Res*. **2013**, *3*, 125–136.

4. Idris, J.; Eyu, G.D.; Mansor, A.M.; Ahmad, Z.; Chukwuekezie, C.S. A preliminary study of biodegradable waste as sorbent material for oil-spill cleanup. *Sci. World J.* **2014**, *2014*, 1–5.
5. Banerjee, S.S.; Joshi, M.V.; Jayaram, R.V. Treatment of oil spill by sorption technique using fatty acid grafted sawdust. *Chemosphere* **2006**, *64*, 1026–1031.
6. Maulion, R.V.; Abacan, S.A.; Allorde, G.G.; Umali, M.C.S. Oil spill adsorption capacity of activated carbon tablets from corncobs in simulated oil-water mixture. *Asia Pac. J. Multidiscip. Res.* **2015**, *3*, 146–151.
7. Aljeboree, A.M.; Alshirifi, A.N.; Alkaim, A.F. Kinetics and equilibrium study for the adsorption of textile dyes on coconut shell activated carbon. *Alex. Eng. J.* **2017**, *10*, S3381–S3393.
8. Anwana Abel, U.; Rhoda Habor, G.; Innocent Oseribho, O. Adsorption studies of oil spill clean-up using coconut coir activated carbon (CCAC). *Am. J. Chem. Eng.* **2020**, *8*, 36–47.
9. Igwegbe, C.A.; Umembamalu, C.J.; Osuagwu, E.U.; Oba, S.N.; Emembolu, L.N. Studies on adsorption characteristics of corn cobs activated carbon for the removal of oil and grease from oil refinery desalter effluent in a downflow fixed bed adsorption equipment. *Eur. J. Sustain. Dev. Res.* **2020**, *5*, 1–14.
10. Atemkeng, C.D.; Anagho, G.S.; Tagne, R.F.T.; Amola, L.A.; Bopda, A.; Kamgaing, T. Optimization of 4-nonylphenol adsorption on activated carbons derived from safou seeds using response surface methodology. *Carbon Trends*. **2021**, *4*, 100052.
11. Silgado, K.J.; Marrugo, G.D.; Puello, J. Adsorption of chromium (VI) by activated carbon produced from oil palm endocarp. *Chem. Eng. Trans.* **2014**, *37*, 721–726.
12. Nguyen, T.T.; Loc, N.D.; Ba, L.H.; Nam, T.V. Efficient oil removal from water using carbonized rambutan peel: Isotherm and kinetic studies. *Vietnam Journal of Hydrometeorology*. **2023**, *4*, 1–18.
13. Hussein, M.; Amer, A. A.; Sawsan, I. I. Oil spill sorption using carbonized pith bagasse: 1. Preparation and characterization of carbonized pith bagasse. *J Anal Appl Pyrolysis*. **2008**, *82(2)*, 205–211.
14. Angelova, D.; Uzunov, I.; Uzunova, S.; Gigova, A.; Minchev, L. Kinetics of oil and oil products adsorption by carbonized rice husks. *J. Chem. Eng.* **2011**, *172(1)*, 306–311.
15. Olufemi, B. A.; Otolorin, F. Comparative adsorption of crude oil using mango (Mangnifera indica) shell and mango shell activated carbon. *Environ. Eng. Res.* **2017**, *22(4)*, 384–392.
16. Oliveira, E.; Santos, J.; Goncalves, A.P.; Mattedi, S.; Jose, N. Characterization of the rambutan peel fiber (nephelium lappaceum) as a lignocellulosic material for technological applications. *Chem. Eng. Trans.* **2016**, *50*, 391–396.
17. Khataee, A.R. Optimization of UV-promoted peroxydisulphate oxidation of C.I. Basic blue 3 using response surface methodology. *Environ. Technol.* **2010**, *31*, 73–86.
18. Draper, N.R.; John, J.A. Response-Surface Designs for Quantitative and Qualitative Variables. *Technometrics*. **1988**, *30*, 423–428.
19. Bayuo, J.; Pelig-Ba, K.B.; Abukari, M.A. Optimization of adsorption parameters for effective removal of lead (II) from aqueous solution. *Phys. Chem.: Indian J.* **2019**, *14*, 1–25.
20. Izevbekhai, O.U.; Gitari, W.M.; Tavengwa, N.T.; Ayinde, W.B.; Mudzielwana, R. Response surface optimization of oil removal using synthesized polypyrrole-silica polymer composite. *Molecules* **2020**, *25*, 4628.

21. Ahmad, M.A.; Alrozi, R. Optimization of rambutan peel based activated carbon preparation conditions for remazol brilliant blue R removal. *J. Chem. Eng*. **2011**, *168*, 280–285.
22. Naderi, M. Chapter fourteen - surface area: brunauer–emmett–teller (BET). Progress in Filtration and Separation. **2015**, pp. 585–608.
23. Mourabet, M.; El Rhilassi, A.; El Boujaady, H.; Bennani-Ziatni, M.; Taitai, A. Use of response surface methodology for optimization of fluoride adsorption in an aqueous solution by Brushite. *Arab. J. Chem.* **2017**, *10*, S3292–S3302.
24. Owolabi, R.U.; Usman, M.A.; Kehinde, A.J. Modelling and optimization of process variables for the solution polymerization of styrene using response surface methodology. *J. King Saud Univ. Eng. Sci.* **2018**, *30*, 22–30.
25. Nnamdi Ekwueme, B.; Anthony Ezema, C.; Asadu, C.O.; Elijah Onu, C.; Onah, T.O.; Sunday Ike, I.; Chinonyelum Orga, A. Isotherm modelling and optimization of oil layer removal from surface water by organic acid activated plantain peels fiber. *Arab. J. Chem*. **2023**, *16*, 104443.
26. NwabuezeH, H.O.; Chiaha, P.N.; Ezekannagha, B.C.; Okoani, O.E. Acetylation of corn cobs using iodine catalyst, for oil spills remediation. *Int. J. Eng. Sci*. **2016**, *5(9)*, 53–59.
27. Vlaev, L.; Petkov, P.; Dimitrov, A.; Genieva, S. Cleanup of water polluted with crude oil or diesel fuel using rice husks ash. *J. Taiwan Inst. Chem. Eng.* **2011**, *42(6)*, 957–964.